Influence of a phonon bath in a quantum dot cavity QED system: Dependence of the shape*

Wang Wei-Sheng(王伟胜), Zhang Ming-Liang(张明亮), and Chen Zhi-De(陈芝得)†

Department of Electronic Engineering, Jinan University, Guangzhou 510632, *China*

(Received 15 January 2014; revised manuscript received 23 February 2014; published online 23 July 2014)

We present a systematic analysis on the role of the quantum dot (QD) shape in the influence of the phonon bath on the dynamics of a QD cavity QED system. The spectral functions of the phonon bath in three representative QD shapes: spherical, ellipsoidal, and disk, are calculated from the carrier wave functions subjected to the confinement potential provided by the corresponding shape. The obtained spectral functions are used to calculate three main effects brought by the phonon bath, i.e., the coupling renormalization, the off-resonance assisted feeding rate and the pure dephasing rate. It is found that the spectral function of a disk QD has the widest distribution, hence the phonon bath in a disk QD can lead to the smallest renormalization factor, the largest dephasing rate in the short time domains(≤ 2 ps), and the off-resonance assisted feeding can support the widest detuning. Except for the pure dephasing rate in the long time domains, all the influences brought by the phonon bath show serious shape dependence.

Keywords: quantum dot, shape dependence, phonon bath, spectral function

PACS: 42.50.Pq, 78.67.Hc, 63.20.kd, 63.22.–m **DOI:** 10.1088/1674-1056/23/9/094205

1. Introduction

Quantum dots (QDs) are the most promising candidates for a variety of applications in future optoelectronic devices[1–4] ranging from single photon sources[5,6] to quantum key encoding[7] and quantum information processing.[8,9] One important issue in the study on QD systems is the influence from the phonon bath on the performance of a QD device. The so-called excitation-induced-dephasing (EID)[10–13] recently found in the Rabi oscillation of a QD system indicates that the phonon bath can bring some unexpected and important influences. In the field of solid state cavity QED, the influence from the phonon bath on the dynamics of a QD microcavity system has been being an interesting subject since the new phenomena were observed in the photoluminescence (PL) spectrum.[14] The intensive study in recent years shows there are mainly three effects brought by the phonon bath: the coupling renormalization, the off-resonance assisted feeding, and the pure dephasing.[15–20] It is known that the influence of a phonon bath can be entirely characterized by its spectral function in theoretical calculations.[21] For the sake of simplicity, most of theoretical study used a spectral function for a QD with spherical symmetry and ignoring the difference between electrons and holes.[10–13,17–19] Nevertheless, it is well known that a real QD is not always of sphere shape, but can be of ellipsoidal shape, disk shape, or other shapes.[1,2] Furthermore, the localization length of the carriers inside a QD is directly related to the effective mass and hence the difference between electrons and holes is always not ignorable.[1,2,22–24] Accordingly, it is reasonable to ask a simple question: how far is the distance from a spherical QD (SQD) with no-difference between electrons and holes to a real QD used in the QD cavity systems? The answer to this question is of critical importance for the comparison between theoretical predictions and experimental observations. In fact, it has been found that, by considering the difference between electrons and holes, the spectral function of a phonon bath can have some special structure which leads to the concept of engineering the phonon scattering.[15] The spectral function of an ellipsoidal QD (EQD) has also been used in Ref. [15]. However, a systematic study on the shape dependence is still lacking and this is the main interest of the present work.

In this paper, the spectral functions of three kinds QD, i.e., the spherical QD, the ellipsoidal QD and the disk QD (DQD), are calculated from the carrier wave functions subject to the confinement potential provided by the corresponding QD shape. It is found that the spectral function is seriously shape-dependent and a simple form can be only found in a spherical QD with no difference between electrons and holes. The spectral function of a disk QD has a much wider distribution than others and is closer to that found by using the so-called 8-band $\boldsymbol{k}\cdot\boldsymbol{p}$ wave function.[25] The obtained spectral functions are used to calculate the influence brought by the phonon bath mentioned above. It is seen that the coupling renormalization factor (also called the Debye–Waller factor[26]) $\langle X\rangle$ decays slowly in a spherical QD while it decays fast in a disk QD with increasing temperature, a result indicates that the phonon-induced Rabi frequency renormalization will be more pronounced in a disk QD than in other QDs, es-

*Project supported by the National Natural Science Foundation of China (Grant No. 10974072).

†Corresponding author. E-mail: tzhidech@jnu.edu.cn

© 2014 Chinese Physical Society and IOP Publishing Ltd

pecially in high-temperature regions. The leading contribution to the off resonance assisted feeding rate is found to be almost independent of the QD shape in the cases of small detuning (lower than 1 meV). However, the decay rate with the increasing detuning shows great difference. For a positive detuning of 5 meV, the feeding rate of a disk QD is about seven-order larger than that of a spherical or ellipsoidal QD, from which we conclude that, to support the off resonance feeding up to a detuning of 5 meV as seen in the experiment,[25,27] a disk QD is the best candidate. The de-phasing rate is also calculated and the result shows that, in low temperature region (say $T < 5$ K), the shape only leads to the difference in very short time domains (≤ 2 ps), while in the experimental observation time domain, the de-phasing rate is almost independent of the QD shape. The organization of the paper is as follows. The definition and the calculation of the spectral function are provided in Section 2, the obtained spectral functions are used to calculate the coupling renormalization factor, the off resonance assisted feeding rate and de-phasing rate in Section 3. Conclusion and discussion are given in Section 4.

2. Spectral function of the phonon bath in a QD

In the low excitation case, a QD can be considered as a two-state system (TSS): the 1-exciton state $|\mathrm{e}\rangle$ and the ground state $|\mathrm{g}\rangle$. Since the phonon energy quantum is much lower than the energy gap of a QD (the latter is about three order larger), the interaction between the QD TSS and the phonon bath can be expressed as[17,18]

$$\hat{H}_{\mathrm{e-ph}} = \hat{\sigma}_{\mathrm{ee}} \sum_{\boldsymbol{q}} \hbar\lambda_{\boldsymbol{q}} (\hat{b}_{\boldsymbol{q}} + \hat{b}^{+}_{\boldsymbol{q}}), \tag{1}$$

where we define $\hat{\sigma}_{ij} = |i\rangle\langle j| (i, j = \mathrm{e}, \mathrm{g})$, $\hat{b}_{\boldsymbol{q}}$ ($\hat{b}^{+}_{\boldsymbol{q}}$) is the annihilation (creation) operator for a phonon with wave vector $\boldsymbol{q}$, and $\lambda_{\boldsymbol{q}}$ is the coupling parameter. For theoretical study on the influence from the phonon bath, the key element is the spectral function defined as[21]

$$J(\omega) = \sum_{\boldsymbol{q}} |\lambda_{\boldsymbol{q}}|^2 \delta(\omega - \omega_q). \tag{2}$$

In a real QD system, the coupling to the optical branch phonon is always ignored in the low temperature regions due to its large energy gap ($\sim$37 meV) of excitation.[16] The contribution from TA phonons is much lower than the LA phonons and hence is also ignored.[17,22,23] On the other hand, the piezoelectric coupling by LA phonons is also neglected since its contribution is much weaker than the deformation potential coupling.[22] For a coupling to LA phonons by deformation potential, the coupling parameter is given by[24]

$$\lambda_{\boldsymbol{q}} = \frac{qD(\boldsymbol{q})}{\sqrt{2\rho\hbar\omega_{\boldsymbol{q}} V}}, \tag{3}$$

where ρ is the mass density, V is the volume, and $D(\boldsymbol{q})$ is the form factor given by

$$D(\boldsymbol{q}) = \int (D_{\mathrm{h}} |\psi_{\mathrm{h}}(\boldsymbol{r})|^2 - D_{\mathrm{e}} |\psi_{\mathrm{e}}(\boldsymbol{r})|^2) \exp(-\mathrm{i}\boldsymbol{q}\cdot\boldsymbol{r}) \mathrm{d}^3 r, \tag{4}$$

with $\psi_{\mathrm{e}}(\boldsymbol{r})$ and $\psi_{\mathrm{h}}(\boldsymbol{r})$ being the wave functions of the electrons and holes, respectively, and $D_{\mathrm{e,h}}$ are the corresponding deformation potential. The confinement potential and the boundary condition of electrons and holes inside a QD depend on the shape of the QD, which leads to a shape-dependent wave function. The shape-dependent wave functions will, through the above equations, lead to shape-dependent $\lambda_{\boldsymbol{q}}$, and hence a shape-dependent spectral function given by Eq. (2). In the following, the spectral functions for three kinds of QD shape, i.e., the spherical QD, the ellipsoidal QD and the disk QD, will be found by using the wave functions subjected to the confinement potential and boundary condition provided by the corresponding QD shape.

It should be noted that the confinement potential used for the calculation of wave function in a QD can be of different types, say, the Gaussian potential,[23] the parabolic potential (also called the harmonic potential),[24] or others.[1] Here we shall take the harmonic potential since it is in agreement with the observed spectrum.[2] For a spherical QD, the ground state wave functions for the electron ($i = \mathrm{e}$) and the hole ($i = \mathrm{h}$) in a harmonic confinement potential are[3]

$$\psi_{\mathrm{S}-i} = \left(\frac{1}{\pi l_i^2}\right)^{3/4} \exp\left(-\frac{r^2}{2l_i^2}\right), \tag{5}$$

where $l_i = \sqrt{\hbar/m_i^* \omega_i}$ is the localization length. Substituting the above wave function into Eq. (4), one can find the spectral function of a spherical QD,

$$J_{\mathrm{S}}(\omega) = \frac{\omega^3}{4\pi^2\hbar\rho u_{\mathrm{L}}^5} \left(D_{\mathrm{h}}^2 \mathrm{e}^{-\omega^2 l_{\mathrm{h}}^2/2u_{\mathrm{L}}^2} + D_{\mathrm{e}}^2 \mathrm{e}^{-\omega^2 l_{\mathrm{e}}^2/2u_{\mathrm{L}}^2} - 2D_{\mathrm{e}} D_{\mathrm{h}} \mathrm{e}^{-\omega^2 (l_{\mathrm{e}}^2 + l_{\mathrm{h}}^2)/4u_{\mathrm{L}}^2} \right), \tag{6}$$

where u_{L} is the longitudinal sound velocity. If we ignore the difference between electrons and holes, i.e., taking $l_{\mathrm{e}} = l_{\mathrm{h}} = l$, the above spectrum function reduces to

$$J_{\mathrm{S}}(\omega) = a\omega^3 \mathrm{e}^{-0.5(\omega/\omega_{\mathrm{c}})^2}, \tag{7}$$

where $a = (D_{\mathrm{h}} - D_{\mathrm{e}})^2 / (4\pi^2\hbar\rho u_{\mathrm{L}}^5)$, and $\omega_{\mathrm{c}} = u_{\mathrm{L}}/l$ is the cutoff frequency. Such a form of spectral function is commonly used in the literature.[10–13,17–19] The coupling constant a depends on the material properties of QD and the cutoff frequency ω_{c} is related to the carrier localization length. Both can be known from the parameters of the QD materials as given in Table 1 for GaAs-type QDs. Here for the sake of comparison, the spectral function used in Ref. [17] with $a = 0.06$ ps^2 and $\hbar\omega_{\mathrm{c}} = 1$ meV will be used as a reference.

For a more realistic condition, the ellipsoidal QD is likely to be found since the confinement potential in the growth direction (setting as the z direction) will be different and usually

stronger than the lateral direction.[2] By setting a different confinement length in the growth direction, the wave function in an ellipsoidal QD can be found

$$\psi_{\mathrm{E}-i} = \left(\frac{1}{\pi L^2}\right)^{1/4} \exp\left(-\frac{z^2}{2L^2}\right) \frac{1}{\sqrt{\pi} l_i} \exp\left(-\frac{x^2+y^2}{2l_i^2}\right), \quad (8)$$

where L is the confinement length in the z direction. Accordingly, the corresponding spectral function is given by

$$\begin{aligned} J_{\mathrm{E}}(\omega) = \frac{\omega^3}{4\pi^2\hbar\rho u_{\mathrm{L}}^5} \Big[& D_{\mathrm{e}}^2 \mathrm{e}^{-\omega^2 l_{\mathrm{e}}^2/2u_{\mathrm{L}}^2} f_{\mathrm{e}}(2l_{\mathrm{e}}^2, \omega) \\ & + D_{\mathrm{h}}^2 \mathrm{e}^{-\omega^2 l_{\mathrm{h}}^2/2u_{\mathrm{L}}^2} f_{\mathrm{e}}(2l_{\mathrm{h}}^2, \omega) \\ & - 2D_{\mathrm{e}}D_{\mathrm{h}} \mathrm{e}^{-\omega^2 (l_{\mathrm{e}}^2+l_{\mathrm{h}}^2)/4u_{\mathrm{L}}^2} f_{\mathrm{e}}(l_{\mathrm{e}}^2+l_{\mathrm{h}}^2, \omega) \Big], \end{aligned} \quad (9)$$

where

$$f_{\mathrm{e}}(x, \omega) = \int_0^1 \exp\left[\frac{\omega^2 t^2 (x - 2L^2)}{4u_{\mathrm{L}}^2}\right] \mathrm{d}t.$$

By setting $l_{\mathrm{e}} = l_{\mathrm{h}} = l$, it can be seen that the leading term contribution of the above spectrum function in the limit $\omega \to 0$ has the form given by Eq. (7).

For a disk shape QD, the confinement potential in the z direction can be considered as an infinite depth potential well of width L, while a harmonic confinement potential is assumed in the lateral plane. In this way, the ground-state wave functions for the electron ($i = \mathrm{e}$) and the hole ($i = \mathrm{h}$) are given by

$$\psi_{\mathrm{D}-i} = \sqrt{\frac{2}{L}} \sin\left(\frac{\pi z}{L}\right) \frac{1}{\sqrt{\pi} l_i} \exp\left(-\frac{x^2+y^2}{2l_i^2}\right), \quad (10)$$

from which one can find the spectral function

$$\begin{aligned} J_{\mathrm{D}}(\omega) = \frac{4\pi^2 u_{\mathrm{L}}}{\hbar\rho} & [D_{\mathrm{h}}^2 f_{\mathrm{d}}\left(2l_{\mathrm{h}}^2, \omega\right) + D_{\mathrm{e}}^2 f_{\mathrm{d}}\left(2l_{\mathrm{e}}^2, \omega\right) \\ & - 2D_{\mathrm{e}}D_{\mathrm{h}} f_{\mathrm{d}}\left(l_{\mathrm{h}}^2 + l_{\mathrm{e}}^2, \omega\right)]. \end{aligned} \quad (11)$$

Here we have defined a function

$$f_{\mathrm{d}}(x, \omega) = \int_0^{\pi} \frac{\omega^3 \sin\theta \left[1 - \cos(\omega L \cos\theta / u_{\mathrm{L}})\right]}{(\omega L \cos\theta)^6 + 16\pi^4 u_{\mathrm{L}}^4 (\omega L \cos\theta)^2 - 8\pi^2 u_{\mathrm{L}}^2 (\omega L \cos\theta)^4} \mathrm{e}^{-\omega^2 x \sin^2\theta / 4u_{\mathrm{L}}^2} \mathrm{d}\theta.$$

When $l_{\mathrm{e}} = l_{\mathrm{h}} = l$, we have

$$J_{\mathrm{D}}(\omega) = \frac{4\pi^2 u_{\mathrm{L}} (D_{\mathrm{h}} - D_{\mathrm{e}})^2}{\hbar\rho} f_{\mathrm{d}}\left(2l^2, \omega\right). \quad (12)$$

It can be seen that, in the present case, the expression is more complicated and an asymptotic function like Eq. (7) is not easy to find.

Table 1. Material parameters for typical GaAs QDs used in our simulations. Parameters which are given without an explicit source are taken from Ref. [20].

Parameter	Value
Mass density, ρ	5370 kg/m^3
Longitudinal sound velocity, u_{L}	5110 m/s
Deformation potential for electrons, D_{e}	−14.6 eV
Deformation potential for holes, D_{h}	−4.8 eV
Exciton–cavity coupling, $\hbar g$	150 μeV
Confinement in z direction, L	4 nm
Confinement in lateral direction of electrons, l_{e}[16]	6.18 nm
Confinement in lateral direction of holes, l_{h}[16]	4.48 nm

By using the parameters given in Table 1, the spectral functions for QDs with different shapes (i.e., the spectral functions given in Eqs. (6), (9), and (11)) can be found and the obtained results are shown in Fig. 1, together with the reference spectral function given by Ref. [17]. As one can see from Fig. 1, the disk-shape QD has the widest distribution and this distribution is closer to the spectral function found by using the so-called 8-band $\boldsymbol{k}\cdot\boldsymbol{p}$ wave function.[25] On the other hand, a local minimum of the spectral function can only be found for a spherical QD, which implies that the concept of engineering the phonon scattering[15] is only suitable for this kind of QD. One can also see that the reference spectral function has much larger peak amplitude, which indicates much stronger electron–phonon interaction strength in the InAs QD than in the GaAs QD.

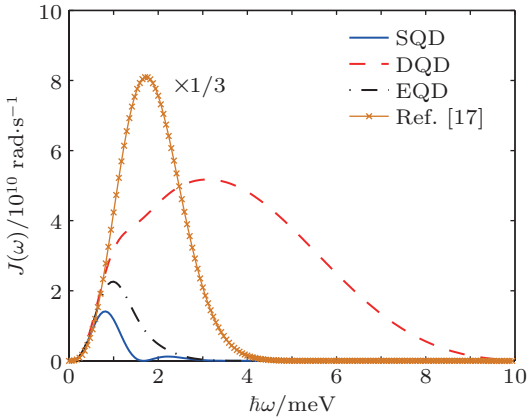


Fig. 1. (color online) Illustration for the obtained spectral functions for different shape QDs by using the parameters given in Table 1. Here SQD represents the spherical quantum dot, EQD and DQD are respectively the ellipsoidal and the disk quantum dot. The reference spectral function used by Ref. [17] is also plotted for comparison.

3. Influence of a phonon bath

In the following, the obtained spectral functions for different shape QDs will be used to calculate the influence from the phonon bath in the corresponding QDs. As we have mentioned before, three representative effects, i.e., the coupling renormalization, the off-resonance assisted feeding rate, and the pure dephasing rate, will be our main interest.

In a QD cavity QED system, the coupling to the phonon bath will lead to the renormalization of the coupling strength between the QD TSS and the cavity mode. Hence, the vacuum Rabi splitting will be modified from Ω to $\langle X\rangle\Omega$,[16–18] where $\langle X\rangle$ is the renormalization factor (also known as the Debye–Waller factor)[26]

$$\langle X\rangle = \exp\left[-\frac{1}{2}\int_0^\infty \frac{J(\omega)}{\omega^2}\coth\left(\frac{\hbar\omega}{2kT}\right)\mathrm{d}\omega\right]. \tag{13}$$

It is obvious that $0 < \langle X\rangle \leq 1$ and larger $\langle X\rangle$ results in smaller renormalization. Since the integrand is an increasing function of temperature, the renormalization factor decreases with increasing temperature. By substituting the obtained spectral functions into the above equation, renormalization factors for different shape QD can be found and the obtained results are shown in Fig. 2. It can be seen that the order of renormalization is as follows: the disk, the ellipsoidal, and the spherical shape QD. The decreasing rate with temperature is found to be less shape-dependent. As one can seen from Fig. 2, the renormalization factor calculated from the reference spectral function is much lower than others, for example, at $T = 60$ K, the renormalization factor of an ellipsoidal QD is about twice the reference one, which means that the modification of the observed vacuum Rabi splitting is about two folds in the later system. This result indicates the importance of an appropriate spectral function for a comparison between theoretical prediction and the experimental observation. As we shall see below, the renormalization factor can also play an important role in the off-resonance assisted feeding rate.

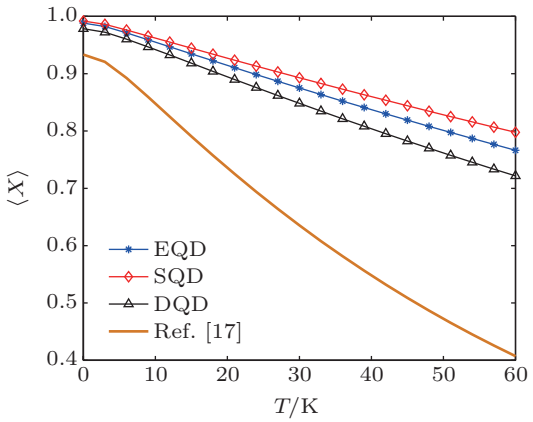


Fig. 2. (color online) Debye–Waller factor as a function of temperature for different QDs. The notation used to specify different shape QDs is the same as in Fig. 1.

We now proceed to study the role of the QD shape on the off-resonance assisted feeding. With the coupling term given by Eq. (1) and using the polaron transformation,[26] off-resonance assisted feeding rate can be found by various methods as given in Ref. [18]. In fact, the total feeding rate can be expressed as a series of contributions from phonon-assisted processes involving different number of phonons. For example, the leading term contribution comes from the process involving 1-phonon, the second term is the contribution from the processes involving 2-phonons, and so on. It is found that, for the detuning lower than 5 meV and the temperature lower than 60 K, the leading term contribution (i.e., the 1-phonon process) makes main contribution to the total feeding rate, and hence we shall take the leading term contribution as the example to show the shape dependence. The leading term contribution from a phonon bath to the off-resonance assisted feeding rate is given by[17,18]

$$\Gamma_1 = 2\pi\left(\frac{g\langle X\rangle}{\Delta}\right)^2 \times \begin{cases} \bar{n}(-\Delta)J(-\Delta), & \Delta < 0, \\ (\bar{n}(\Delta)+1)J(\Delta), & \Delta > 0, \end{cases} \tag{14}$$

where g and Δ are respectively the coupling strength and the detuning between the QD TSS and the cavity mode, $\bar{n}(\omega)$ is the Bose–Einstein distribution

$$\bar{n}(\omega) = \frac{1}{\exp(\hbar\omega/kT)-1}$$

at temperature T, and k is the Boltzmann constant.

The obtained Γ_1 for different shape QDs at two representative temperatures ($T = 2$ K and 20 K) are shown in Fig. 3. As one can see from Fig. 3, in the cases of small detuning when $|\Delta| \leq 1$ meV, Γ_1 is almost independent of the QD shape. Nevertheless, the deceasing rate of Γ_1 with increasing Δ shows serious shape dependence. It can be seen that the deceasing rate of a disk QD is much lower than the other two QDs. When the detuning increases to about 5 meV, the feeding rate of a disk QD is about seven order larger than that of a spherical or ellipsoidal QD. This result indicates that the QD shape plays an important role in the large detuning case, and to support an off-resonance feeding up to 5 meV as seen in the experiments,[25,27] the disk shape QD is the best candidate. It can also be seen that the quenching of phonon-induced processes[15] only appears in a spherical QD as we have known from the obtained spectral function shown in Fig. 1. One can find that Γ_1 shows serious temperature dependence in the negative detuning regime, while in the positive detuning regime, Γ_1 is less temperature-dependent.

To see the relation between the renormalization factor and the off-resonance assisted feeding rate, the leading term contribution Γ_1 for an SQD and that calculated from the reference spectral function are shown in Fig. 4. The obtained result shows that the peak value of the SQD is about two times larger than the reference model. This is mainly due to the fact that the renormalization factor of the reference model is about two times lower than the SQD (see Fig. 2). It can also be seen that the reference model can support a detuning about two times larger than the SQD. It should be noted that, in a real

experiment, the assisted feeding rate cannot be observed directly. Instead one can measure the spontaneous emission lifetime, which can be extracted from the assisted feeding rate by quantum-kinetic simulations of the master equation.[28] Obviously, the difference between these two models can be seen in the extracted lifetime and this result again indicates the importance of using an appropriate spectral function to understand the experimental observation.

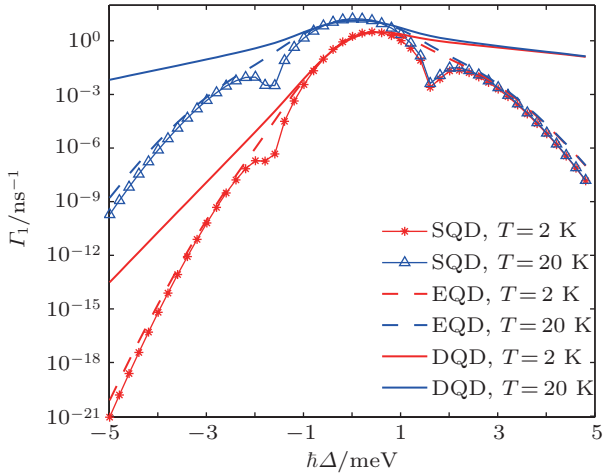


Fig. 3. (color online) Leading term contribution of the off-resonance assisted feeding rate for different shape QDs at two representative temperatures: $T = 2$ K (red) and $T = 20$ K (blue). The notation used to specify different shape QDs is the same as that in Fig. 1.

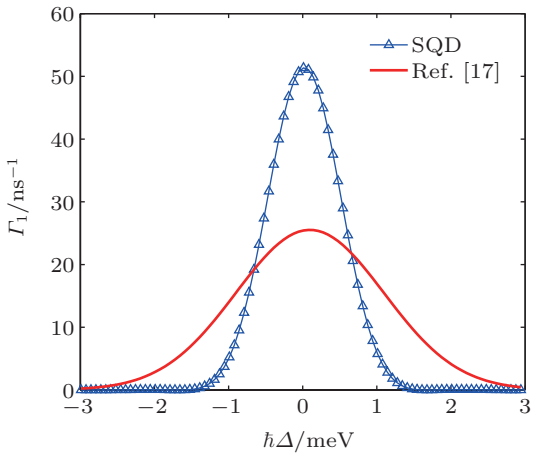


Fig. 4. (color online) Comparison of the leading term off-resonance assisted feeding rate between the SQD model (Eq. (6)) and the reference model at temperature $T = 60$ K.

We now proceed to investigate the dependence of the QD shape on phonon-induced pure dephasing rate. Since our main interest is the QD cavity QED system, the EID-like dephasing rate will not be calculated, instead the pure dephasing rate based on the perturbation treatment will be used as the example to see the shape dependence. In the case of resonance, the phonon-induced pure dephasing rate is given by[16]

$$\gamma_{\mathrm{ph}}(t) = \int_0^t \cos(2g\tau)\mathrm{Re}\,[D(\tau)]\,\mathrm{d}\tau, \tag{15}$$

where $D(t)$ is the phonon bath correlation function

$$\mathrm{Re}\,[D(t)] = \int_0^\infty J(\omega)\cos(\omega t)\coth\left(\frac{\hbar\omega}{2kT}\right)\mathrm{d}\omega. \tag{16}$$

Solving Eqs. (15) and (16), the pure dephasing rate for three different shape QDs at $T = 4$ K is plotted in Fig. 5. We find that, in the low temperature region of $T < 5$ K, the shape dependence can only be found in a very short time domain (≤ 2 ps), and at this time domain the disk QD has a much higher pure dephasing rate than other QDs. As one can see from Fig. 1, the disk QD has the widest distribution of interaction frequency range, and at the beginning, $\gamma_{\mathrm{ph}}(t)$ is determined by the bare QD–phonon coupling with the full phonon spectrum,[15] hence the dephasing rate in a short time regime has the largest value. Interestingly, on the long time scale, the pure dephasing rates of all the three different shape QDs approach the same constant value, a result shows that, in the experimental observation time domains, the dephasing rate becomes shape-independent. As a matter of fact, the dephasing rate calculated in this way mainly comes from the contribution of the phonon modes in resonance with the Rabi oscillation.[10] As one can see from Fig. 1, the spectral functions for all three kinds of QDs are almost the same in the regions of $\hbar\omega < 1$ meV. Since the Rabi oscillation frequency is lower than 1 meV, the contribution of phonon modes in resonance with the Rabi oscillation is almost shape-independent. It should also be noted that, at higher temperature (say $T > 10$ K), the dephasing rate will become shape-dependent though the dependence is not very serious.

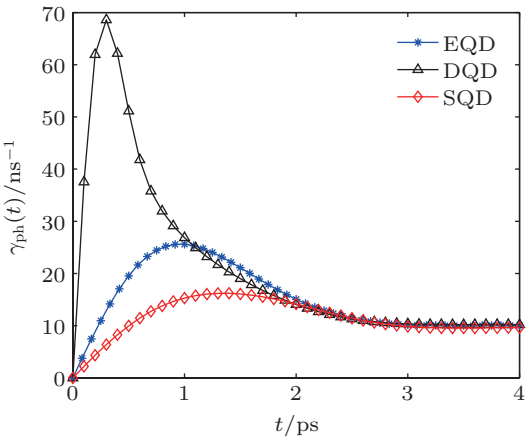


Fig. 5. (color online) Time evolution of phonon-induced pure dephasing rate for different shape QDs at $T = 4$ K. The notation used to specify the different shape QDs is the same as that in Fig. 1.

4. Conclusion and discussion

We have presented a systematic analysis on the role of the QD shape in the influence of the phonon bath on the dynamics of a QD cavity QED system. The spectral functions of the phonon bath in three representative QD shapes, i.e., spherical, ellipsoidal, and disk shape, are calculated from the carrier wave functions subjected to the confinement potential

provided by the corresponding shape. The obtained spectral functions are used to calculate three main effects brought by the phonon bath, i.e., the coupling renormalization, the off-resonance assisted feeding rate and the pure dephasing rate. It is found that the spectral function of a disk QD has the widest distribution, hence the phonon bath in a disk QD can lead to the smallest renormalization factor, the largest dephasing rate in the short time domains (≤ 2 ps), and the off-resonance assisted feeding can support the widest detuning. Except for the pure dephasing rate in the long time domains, all the influences brought by the phonon bath show serious shape dependence. The comparison with the reference spectral function indicates the importance of using the appropriate spectral function to understand the experimental observation. The present work provides the exact way to calculate the spectral function of the phonon bath in a QD on one hand, and on the other hand, it also gives theoretical guides for engineering based on the phonon scattering processes.

Acknowledgment

Wang Wei-Sheng acknowledges Prof. P. Kaer for helpful discussion.

References

[1] Williamson A J 2002 *Quantum Dots* (Singapore: World Scientific) p. 15
[2] Petroff P M 2003 *Single Quantum Dots* (Berlin: Springer-Verlag) p. 1
[3] Fox M 2006 *Quantum Optics: An Introduction* (Oxford: Oxford University Press) p. 333
[4] Li X K, Jin P, Liang D C, Wu J and Wang Z G 2013 *Chin. Phys. B* **22** 048102
[5] Niu Z C, Sun B Q, Dou X M, Xiong Y H, Wang H L, Ni H Q, Li S S and Xia J B 2010 *Physics* **39** 737 (in Chinese)
[6] Michler P, Kiraz A, Becher C, Schoenfeld W V, Petroff P M, Zhang L D, Hu E and Imamoğlu A 2000 *Science* **290** 2282
[7] Stevenson R M, Thompson R M, Shields A J, Farrer I, Kardynal B E, Ritchie D A and Pepper M 2002 *Phys. Rev. B* **66** 081302
[8] Chen W, Xue Z Y, Wang Z D and Shen R 2014 *Chin. Phys. B* **23** 030309
[9] Troiani F, Molinari E and Hohenester U 2003 *Phys. Rev. Lett.* **90** 206802
[10] Ramsay A J, Gopal A V, Gauger E M, Nazir A, Lovett B W, Fox A M and Skolnick M S 2010 *Phys. Rev. Lett.* **104** 017402
[11] Ramsay A J, Godden T M, Boyle S J, Gauger E M, Nazir A, Lovett B W, Fox A M and Skolnick M S 2010 *Phys. Rev. Lett.* **105** 177402
[12] Ramsay A J, Godden T M, Boyle S J, Gauger E M, Nazir A, Lovett B W, Gopal A V, Fox A M and Skolnick M S 2011 *J. Appl. Phys.* **109** 102415
[13] McCutcheon D P S and Nazir A 2010 *New J. Phys.* **12** 113042
[14] Hennessy K, Badolato A, Winger M, Gerace D, Atatüre M, Gulde S, Fält S, Hu E L and Imamoğlu A 2007 *Nature* **445** 896
[15] Nysteen A, Kaer P and Mork J 2013 *Phys. Rev. Lett.* **110** 087401
[16] Kaer P, Nielsen T R, Lodahl P, Jauho A P and Mørk J 2012 *Phys. Rev. B* **86** 085302
[17] Hughes S, Yao P, Milde F, Knorr A, Dalacu D, Mnaymneh K, Sazonova V, Poole P J, Aers G C, Lapointe J, Cheriton R and Williams R L 2011 *Phys. Rev. B* **83** 165313
[18] Roy C and Hughes S 2011 *Phys. Rev. X* **1** 021009
[19] Xue J, Zhu K D and Zheng H 2008 *J. Phys.: Condens. Matter* **20** 325209
[20] Hohenester U 2010 *Phys. Rev. B* **81** 155303
[21] Leggett A J, Chakravarty S, Dorsey A T, Fisher M P A, Anupam G and Zwerger W 1987 *Rev. Mod. Phys.* **59** 1
[22] Krummheuer B, Axt V M and Kuhn T 2002 *Phys. Rev. B* **65** 195313
[23] Takagahara T 1999 *Phys. Rev. B* **60** 2638
[24] Calarco T, Datta A, Fedichev P, Pazy E and Zoller P 2003 *Phys. Rev. A* **68** 012310
[25] Stock E, Dachner M R, Warming T, Schliwa A, Lochmann A, Hoffmann A, Toropov A I, Bakarov A K, Derebezov I A, Richter M, Haisler V A, Knorr A and Bimberg D 2011 *Phys. Rev. B* **83** 041304
[26] Mahan G D 2000 *Many Particle Physics* (3th edn.) (New York: Plenum Press) p. 461
[27] Dalacu D, Mnaymneh K, Sazonova V, Poole P J, Aers G C, Lapointe J, Cheriton R, Thorpe A J S and Williams R 2010 *Phys. Rev. B* **82** 033301
[28] Hohenester U, Laucht A, Kaniber M, Hauke N, Neumann A, Mohtashami A, Seliger M, Bichler M and Finley J J 2009 *Phys. Rev. B* **80** 201311